# ENVIRONMENT DEPENDENT TRANSITION FREQUENCIES FOR RAM AND BELLHOP

Iris E. Hartstra[a], Erik Salomons[a], Mathieu E.G.D. Colin[a] and Mark K. Prior[a]

[a] TNO, Oude Waalsdorperweg 63, 2597 AK The Hague, THE NETHERLANDS

***Abstract:*** *Passive-sonar-performance modelling requires the accurate estimation of the acoustic field for a broad range of frequencies in various environments. In this paper, we assess the suitability of a Gaussian Beam (Bellhop) and Parabolic Equation model (RAM), whereby we focus primarily on computational efficiency.*
*For Parabolic Equation (PE) models the computation time increases with the number of grid-points required to provide accurate results. Since the grid-size scales to the wavelength, the computation time generally increases with frequency. The computation time of Gaussian Beam models increases primarily with longer maximum range. Since lower frequencies result in relevant acoustic intensities at larger distances, this results in a computation time increase in case of lower frequencies.*
*Our aim is to estimate a single-run 'transition frequency' that determines which model is optimal in terms of computational costs, while ensuring that each model is subjected to a convergence criterion we set at 1 dB. We only consider single-frequency runs in this paper. The transition frequencies are estimated for three different scenarios that vary in depth and sound speed profile (SSP). We find that RAM is the computationally efficient choice up to a transition frequency of about 11 kHz and 12 kHz in the case of the shallow water scenarios: Weston Case 1 and 4, respectively. For the deep water scenario, a Munk profile truncated at 1 km depth, RAM is found to be the most efficient choice up to about 4.5 kHz.*

***Keywords:*** *sonar performance, computation time, parabolic equation model, Gaussian beam model, transition frequency*

## 1. INTRODUCTION

Passive-sonar-performance modelling is required to estimate the ability of a passive sonar system to detect a target in an operational environment. These models aim to provide reliable spatial maps of probability of detection within an acceptable length of computation time. In recent years, the bandwidth of hydrophones has increased significantly, especially towards the higher frequency range. This advancement demands a reassessment of the operational practicality of different acoustic propagation models as a function of frequency and environmental parameters (such as water depth).

In this paper we compare two widely used and benchmarked models that are based on distinct physical approximations: the Gaussian Beam (GB) model of Bellhop [1] and the Parabolic Equation (PE) model RAM [2].

Gaussian Beams are solved in a two-step approach, of which the first entails the numerical integration of ray trajectories throughout the medium and the second the computation of the associated intensity along and in the vicinity of the rays. The coherent form of Gaussian Beams has a low frequency limitation in terms of computation time, because the accurate reconstruction of model interference patterns at low frequencies requires a very large number of rays. The computation time of both coherent and incoherent GB models increases with increasing propagation distance, because the ray trajectories are traced further out. This will lead to a longer computation time for lower frequencies, because lower frequency waves are less affected by absorption and thus propagate further out than high frequency waves. In this paper, we will use the incoherent form of Bellhop, because we consider acoustic intensities.

The PE model solves the full one-way wave equation by marching an initial field solution (the starter field), resolved for all depths at zero range, in the range direction. Since the 'marching steps' are a function of wavelength, we expect the computation time of this model to increase with frequency. However, as in the case of GB models, we expect this effect to be curbed by the fact that the maximum range at which PL values remain relevant is lower for higher frequencies.

We conduct convergence tests and depth-averaged intensity comparisons to closed-form solutions for three different scenarios, of which the first two are based on examples of the Weston Memorial Workshop: the Weston Case 1 is a homogeneous Pekeris waveguide with 100 metre water depth [3], and the Weston Case 4 is the same as 1, but contains a wedge that linearly rises to a depth of 30 metres between 5 and 7 km range [3]. The third scenario is a deep water environment: we adapt the original Munk profile [4] by placing the bottom at 1 km depth. We use the same environmental parameters (e.g. coarse-grained sediment, SSP, etc.) as described in [5]. However, instead of having a constant maximum range, we vary the maximum range as a function of frequency in order to limit the propagation loss (at maximum range) to values that are rendered relevant for sonar applications (~75-100 dB re $m^2$). The frequencies we consider are 100, 500, 1000, 4000, 10000, 15000 and 20000 Hz. By monitoring the computation time of the respective models as a function of these frequencies, we aim to estimate a single-run transition frequency for each environmental scenario.

# 2. THEORY

## 2.1. Parabolic Equation model

The Parabolic Equation model (PE model) is an efficient numerical method for calculating sound propagation from a point source to a distant receiver in a refracting medium [6]. The sound pressure field is calculated as a function of range and depth on a rectangular grid. The PE model can be used for situations with range-dependent medium properties. The field is calculated in steps along the range axis. A change of a medium property at a certain range is taken into account by a change in the parameters of the propagation formulas. Of practical interest is range dependence of the sound speed profile and the water depth. It should be emphasized that the PE model is not subject to a high-frequency approximation (which is the case for ray models), so PE is particularly useful and efficient for sound propagation at lower frequencies.

For the study described in this paper we employed the efficient split step Padé PE model developed by Collins [7]. We make use of a Fortran version of this PE model, which is referred to as RAM PE (RAM stands for Range-dependent Acoustic Model) [2].

## 2.2. Gaussian Beam model

The full derivation of the Helmholtz equation can be formulated in terms of an infinite series of equations [1,6]. The governing equation for the Gaussian Beam model follows by considering two main equations of this series: the Eikonal equation (ray or travel time solutions), and the transport equation (intensity).

In a first step, the Eikonal equation is solved, yielding a ray fan which provides travel time and ray angle information throughout the medium and represents a 'high-frequency approximation' of the acoustic field. The bending of the rays is controlled by the variations in sound speed of the medium according to Snell's law.

In the next step, the transport equation is solved to obtain a solution for the amplitude of the acoustic pressure field along the rays, which varies due to geometrical spreading and focusing. The amplitude in the vicinity of the ray can be derived by taking the ray central axis as maximum value and decreasing it by a Gaussian shape in the perpendicular direction from the ray axis. The width of this Gaussian shape is computed by the dynamic ray equations, which are a function of the local ray density and sound speed variations. The intensity distribution, obtained by summing the resulting beams, respects low frequency effects such as shadow zones and is unaffected by caustics [1].

## 2.3. Closed-form solutions

We compare the PL calculations of Bellhop and RAM with closed-form expressions that are based on mode-stripping. These expressions can be rigorously simplified by using the fact that higher order modes experience more attenuation [8]). We use the range-independent closed-form expression from [8] (Eq. 4 in [8]) for the range-independent cases 1 and 3. For the range-dependent case 4, we use the range-dependent closed-form expression from [9] (Eq. 21 in [9]).

## 3. EXPERIMENTS

For the three different scenarios defined in the introduction we run both RAM and Bellhop for different frequencies (first row in Table 1). To prevent the intensity of the acoustic field to reach values that are rendered insignificant for sonar applications, we allow the maximum range to vary as a function of frequency using an empirical relation (second row in Table 1). The fact that Bellhop has the option to calculate only an incoherent solution allows us to use a larger grid-size in the vertical direction, which saves computation time. For RAM we use the Nyquist criterion to define the grid-size in the vertical direction (remaining rows of Table 1). Both models are subjected to convergence tests for each different scenario and frequency. The model settings that result in a convergence within a criterion of 1 dB are used for the experiments that serve to estimate the transition frequency. This criterion provides sufficient practical accuracy, because it is a small value when compared to the uncertainty of environmental input data as discussed in [10]. The (possible) intersection of the computation time of Bellhop and RAM will serve to interpret the transition frequency.

**Table 1: The maximum range varies as function of frequency. The vertical grid-size for Bellhop's receiver output grid varies by scenario, whereas for RAM it varies as function of frequency: it is equal to the spatial Nyquist criterion.**

| Frequency [Hz] | | 100 | 500 | 1000 | 4000 | 10000 | 15000 | 20000 |
|---|---|---|---|---|---|---|---|---|
| MaxRange [km] | | 200 | 76 | 50 | 22 | 13 | 10 | 8 |
| Bell dzOut [m] | Scen 1 | 2 | 2 | 2 | 2 | 2 | 2 | 2 |
| | Scen 2 | 2 | 2 | 2 | 2 | 2 | 2 | 2 |
| | Scen 3 | 10 | 10 | 10 | 10 | 10 | 10 | 10 |
| RAM dzOut [m] | | 7.5 | 1.5 | 0.75 | 0.1875 | 0.075 | 0.05 | 0.0375 |

### 3.1. Convergence tests

The RAM PE model has several numerical parameters, which must be optimized in order to achieve accurate results in an efficient way. Important parameters are the horizontal and vertical grid-sizes $\Delta r$ and $\Delta z$ of the computation grid. We found that the horizontal grid-size $\Delta r$ may be chosen as large as $10\lambda$ (where $\lambda$ is the wavelength), for frequencies in the range 50-4000 Hz. For the vertical grid-size $\Delta z$ smaller values must be used, ranging from $0.1\lambda$ at 50 Hz to $1.0\lambda$ at 4000 Hz.

These optimized values were determined by convergence tests where the depth-averaged propagation loss was considered as a function of range. Due to the complex nature of PE convergence, we limited the test method to a visual assessment. The criterion was that the propagation loss should not change by more than about 1 dB if smaller values were used for the horizontal and vertical grid-size. We found that choosing the vertical grid-size too small, smaller than $0.01\lambda$, led to inaccurate results.

There were also other numerical parameters which we varied in the convergence tests. These include: i) the number of Padé terms (we used 8 terms for the calculations reported here), ii) the thickness of the sediment (we used $20\lambda$ for the calculations reported here), and iii) some parameters of the absorption layer below the sediment (we followed the approach described in [6]). For the convergence tests we also considered the results of convergence tests performed by [9] and [11].

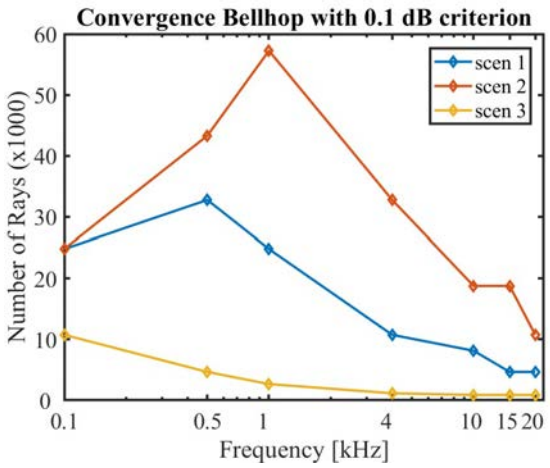


**Figure 1a Number of rays required per frequency and scenario for Bellhop to converge within 0.1 dB. NB: different y axis limits are used than in figure 1b.**

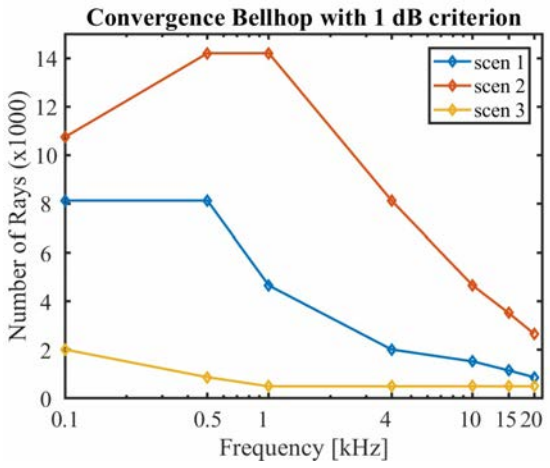


**Figure 1b Number of rays required per frequency and scenario for Bellhop to converge within 1 dB. NB: different y axis limits are used than in figure 1a.**

For the Gaussian Beam model, Bellhop, we determine the optimal number of rays necessary to reach convergence of the depth-averaged PL at one kilometre short of the maximum range. Figure 1a shows the convergence results for a criterion of 0.1 dB. However, we use the number of rays that yields a convergence of 1 dB (Figure 1b) for the experiments conducted in this paper to determine the transition frequency per scenario.

### 3.2. Relative depth averages

For the first scenario at 100 Hz, the depth-averaged results of RAM deviate from the closed-form solution by less than 1 dB for ranges up to about 35 km, beyond which RAM starts to increasingly deviate, reaching a value of about 6 dB at the maximum range of 200 km (Figure 2a). Bellhop deviates between 1-2 dB until about 130 km, beyond which it reaches a deviation of about 3 dB at 200 km range. At 4000 Hz both RAM and Bellhop hardly deviate. For the second scenario: at 100 Hz, both Bellhop and RAM differ significantly from the closed form solution: RAM by about 3 dB in the 100-metre-deep zone, which increases to more than 6 dB for the 30-metre-deep zone, and Bellhop by about 1 dB in the 100-metre-deep zone, which increases to about 6 dB in the 30-metre-deep zone (Figure 2c). At 4000 Hz, both models do not deviate from the closed-form solution by more than a dB (Figure 2d).

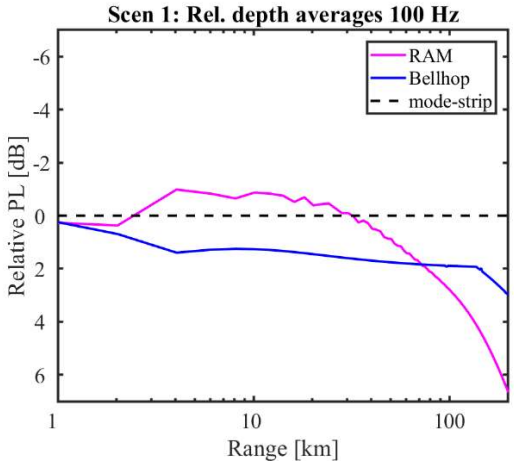


**Figure 2a**

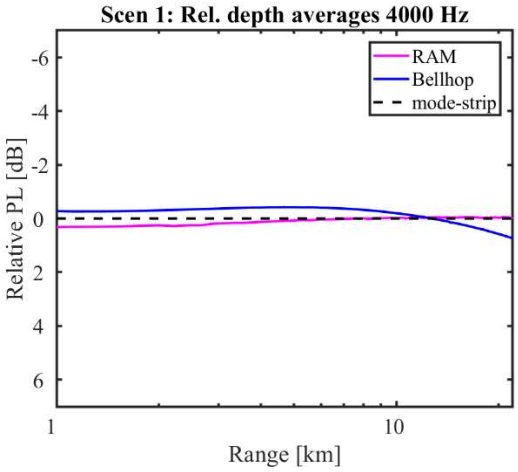


**Figure 2b**

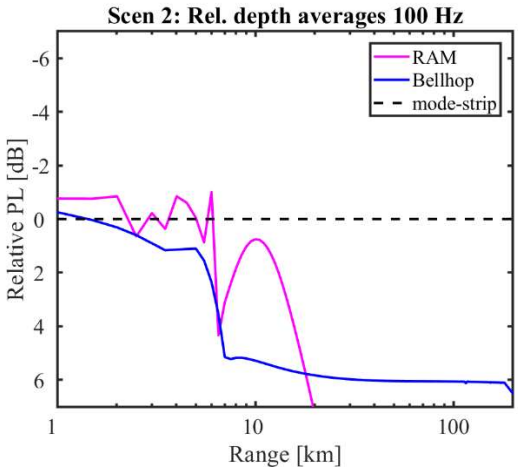


**Figure 2c**

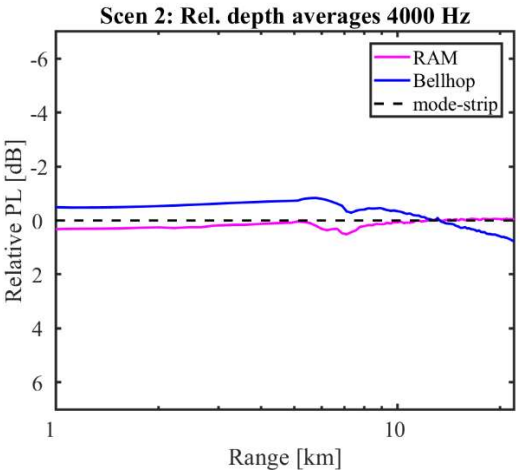


**Figure 2d**

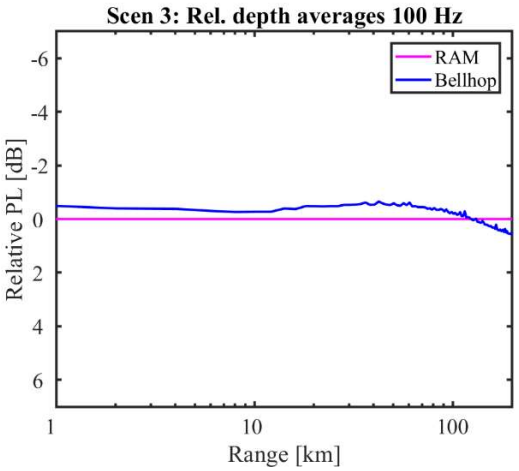


**Figure 2e**

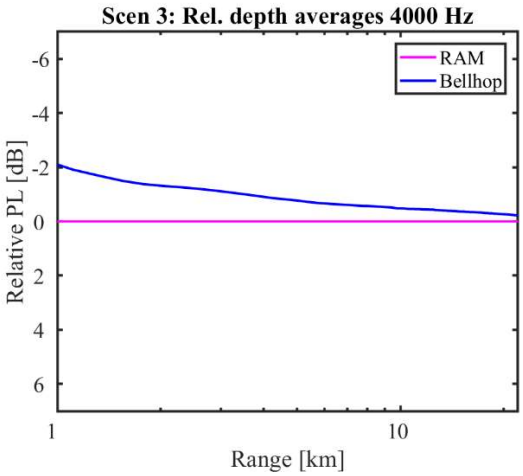


**Figure 2f**

**Figure 2 Figures a-d show depth-averaged PL with respect to the closed-form solutions for the two Weston scenarios for 100 and 4000 Hz. Not that the maximum range varies as a function of frequency (see Table 1). Figures e and f show depth-averaged PL of Bellhop with respect to RAM for the deep water scenario.**

For the third scenario, we only analyzed the averaged PL difference between the two models, because we do not have a closed-form solution for a Munk profile. For 100 Hz, the models give almost the same result, while for 4000 Hz Bellhop deviates by about 2 dB from RAM for the smaller ranges (Figures 2e and 2f, respectively).

### 3.1. Single-run transition frequency

We estimate the transition frequency by comparing the computation times of both models for a single-frequency run. The transition frequency per scenario is defined as the frequency above which RAM has a longer computation time than Bellhop, and thus becomes less practical for single-frequency applications. Table 2 displays the single-run transition frequencies we found per scenario number. Figure 3 shows how the transition frequency is estimated from the intersection of the two computation time curves of Bellhop and RAM for the deep water scenario: the intersection occurs around 4.5 kHz.

**Table 2 Single-run transition frequency estimates for each scenario.**

| Scenario | Transition Frequency [kHz] |
|---|---|
| 1 Weston | 11 |
| 2 Weston, wedge | 12 |
| 3 Deep water | 4.5 |

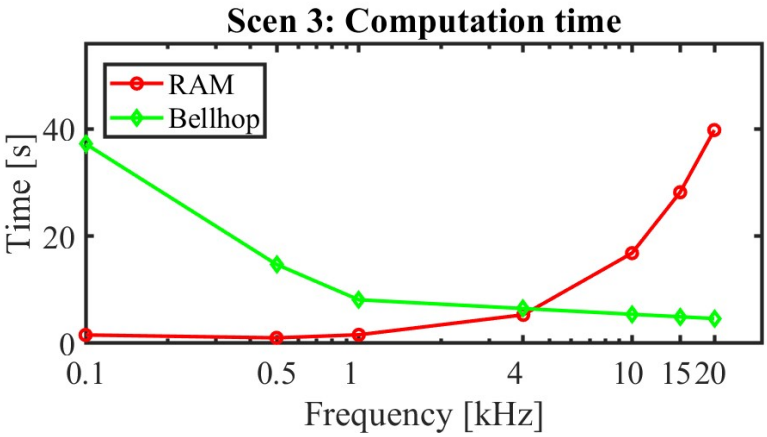


**Figure 3 Computation time for a single-frequency run of RAM and Bellhop for the deep water scenario 3. The intersection occurs around 4.5 kHz, which is interpreted as the single-run transition frequency for this scenario.**

## 4. DISCUSSION AND CONCLUSIONS

Both Bellhop and RAM deviated from the closed-form solution in some of the cases considered. The deviations for Bellhop were especially large for the Weston Case 4 (wedge) at 100 Hz in the 30-metre-deep zone. In this same scenario, RAM shows the largest deviation as well and to a greater extent than Bellhop. This specific example may indicate an issue with the use of single precision the *fortran* version of the RAM code. The single-

run transition frequencies displayed in Table 2 show that RAM is the most efficient choice in the case of scenarios 1 and 2 for frequencies up to about 12 kHz. However, in the case of deep water, Bellhop is more efficient than RAM above a frequency of 4.5 kHz. This is expected, because RAM requires considerable more grid-points for computing deep water solutions.
As a final note, we emphasize that the transition frequencies we present in this paper are only valid for single-frequency runs. When for instance time resolution is required, the transition frequencies could turn out to be very different, because multiple frequency runs are necessary in this case for RAM [3].

**Acknowledgement**
This work was sponsored by the Defence Materiel Organisation of The Netherlands.

## REFERENCES

[1] **Porter, M. B. and Bucker, H. P.** (1987). Gaussian beam tracing for computing ocean acoustic fields. The Journal of the Acoustical Society of America, 82(4), 1349-1359.
[2] Fortran code for RAM PE by M. Collins and is available at the Open Acoustics Library, http://oalib.hlsresearch.com/PE/RAM/. The code is called ram.f, version 1.5.
[3] **M. Zampolli, M. A. Ainslie, P. Schippers** (2010). Scenarios for benchmarking range-dependent active sonar performance models. *Ainslie, MA, Validation of Sonar Performance Assessment Tools: In Memory of David E Weston,* 2010
[4] **Munk, W. H.** (1974). Sound channel in an exponentially stratified ocean, with application to SOFAR. The Journal of the Acoustical Society of America, 55(2), 220-226.
[5] **H.Ö. Sertlek, M.A. Ainslie, K.D., Heaney** (2018). Analytical and Numerical Propagation Loss Predictions for Gradually Range-Dependent Isospeed Waveguides. *IEEE Journal of Oceanic Engineering.*
[6] **F.B. Jensen, W.A. Kuperman, M.B. Porter, H. Schmidt,** "Computational Ocean Acoustics", Springer, 2011
[7] **M.D. Collins**, "A split-step Padé solution for the parabolic equation method", J. Acoust. Soc. Am. **93**, 1736–1742 (1993).
[8] **C.H. Harrison** (2003). Closed-form expressions for ocean reverberation and signal excess with mode stripping and Lambert's law. *J. Acoust. Soc. Am. 114 (5)*
[9] **H.Ö. Sertlek and M.A. Ainslie**, "Propagation loss model comparisons on selected scenarios from the Weston Memorial Workshop", *Proc. first international conference and exhibition on underwater acoustics, UAC 2013, Corfu, Greece.*
[10] **B. Binnerts, C. de Jong, I. Karasalo, M. Östberg, T. Folegot, D. Clorennec, M. Ainsley, A. MacGillivray, G. Warner, L. Wang,** "Model benchmarking results for ship noise in shallow water", *Proc. fifth international conference and exhibition on underwater acoustics, UAC 2019, Hersonissos, Greece*
[11] **E.T. Küsel and M. Siderius,** "Comparison of propagation models for the characterization of sound pressure fields", *IEEE Journal of Oceanic Engineering, DOI 10.1109/JOE.2018.2884107*